

Quenching of rotationally excited CO by collisions with H₂

Benhui Yang* and P. C. Stancil†

Department of Physics and Astronomy and the Center for Simulational Physics

The University of Georgia, Athens, Georgia 30602-2451

N. Balakrishnan‡

Department of Chemistry, The University of Nevada, Las Vegas, Nevada 89154

R. C. Forrey§

Department of Physics, Penn State University,

Berks-Lehigh Valley College, Reading, Pennsylvania 19610

Abstract

Quantum close-coupling and coupled-states approximation scattering calculations of rotational energy transfer in CO due to collisions with H₂ are presented for collision energies between 10⁻⁶ and 15,000 cm⁻¹ using the H₂-CO interaction potentials of Jankowski and Szalewicz [J. Chem. Phys. **123**, 104301 (2005); **108**, 3554 (1998)]. State-to-state cross sections and rate coefficients are reported for the quenching of CO initially in rotational levels $j_2 = 1 - 3$ by collisions with both para- and ortho-H₂. Comparison with available theoretical and experimental results shows good agreement, but some discrepancies with previous calculations using the earlier potential remain. Interestingly, elastic and inelastic cross sections for the quenching of CO($j_2 = 1$) by para-H₂ reveal significant differences at low collision energies. The differences in the well depths of the van der Waals interactions of the two potential surfaces lead to different resonance structures in the cross sections. In particular, the presence of a near-zero energy resonance for the earlier potential which has a deeper van der Waals well yields elastic and inelastic cross sections that are about a factor of 5 larger than the newer potential at collision energies lower than 10⁻³ cm⁻¹.

*Electronic address: yang@physast.uga.edu

†Electronic address: stancil@physast.uga.edu

‡Electronic address: naduvala@unlv.nevada.edu

§Electronic address: rcf6@psu.edu

I. INTRODUCTION

Rotationally-inelastic collisions of molecular species by atoms and molecules, so-called rotational energy transfer, is an important process in a variety of astrophysical environments including interstellar clouds, photodissociation regions (PDRs), and cool stellar/planetary atmospheres. Inherent in the majority of model atmosphere/synthetic spectra studies is the assumption of local thermodynamic equilibrium (LTE), i.e. that the level populations of the atoms and molecules can be described by a Boltzmann distribution. There is reason to suspect departure from LTE in extrasolar giant planets (EGPs) and cool dwarf stars, such as brown dwarfs (BDs), due to a low abundance of electrons and the strong irradiation from their companion stars [1]. Rotational and vibrational level populations are also found to depart from LTE in PDRs due to electronic excitation from stellar UV irradiation and subsequent fluorescence [2, 3]. However, gas modeling and spectral synthesis of EGPs, BDs, PDRs, and other cool astrophysical environments require an extensive array of accurate molecular data including state-to-state rate coefficients. A large portion of the data are either currently unavailable or the available data are insufficient to meet the modeling application demands. Comprehensive experimental and theoretical studies of such processes are now becoming feasible.

Due to their astrophysical importance as H_2 and CO are the most abundant molecules in a broad spectrum of astrophysical objects, the H_2 - CO collisional system has been the subject of numerous experimental [4–17] and theoretical [17–35] studies. Quantitative determinations of state-to-state cross sections and rate coefficients for H_2 - CO collisions are crucial to numerical astrophysical models. However, as measurements of these quantities are difficult, numerical models often rely on cross sections and rate coefficients derived from theoretical calculations. Green *et al.* [18] performed close-coupling calculations of rate coefficients based on an approximate H_2 - CO potential surface in 1976. Since then, a number of quantum scattering calculations were carried out on various potential energy surfaces (PESs).

Accurate potential surfaces for the H_2 - CO complex are needed for reliable theoretical simulations of energy transfer in H_2 - CO collisions. A number of PESs [19–23, 25, 26] have been developed for the H_2 - CO complex over the years. Among these surfaces, Schinke and co-workers [23] extended the rigid rotor H_2 - CO PES [22] to nonequilibrium CO bond

distances, but still treating the dimer as rigid. This surface allows study of vibrationally inelastic processes, which was used by Bacić *et al.* [23, 24] to investigate the vibrational relaxation of CO ($v = 1$) in collisions with H₂ including the rotational degree of freedom of H₂. Reid *et al.* [31] also investigated the vibrational deactivation of CO ($v = 1$) by inelastic collisions with H₂ using this surface.

In 1998, Jankowski and Szalewicz [25] reported a four-dimensional PES for the H₂-CO system. This potential, referred to as V₉₈, was calculated using the symmetry-adapted perturbation theory (SAPT) method with high-level electron correlation effects. Antonova *et al.* [17] calculated state-to-state cross sections of rotational excitation of CO by H₂ at collision energies of 795.0, 860.0, and 991.0 cm⁻¹ on the V₉₈ surface. They also reported experimental results of rotational excitation of CO by H₂ at the same collision energies and obtained good agreement with the theoretical predictions. Gottfried and McBane [36] calculated the second virial coefficients for mixtures of hydrogen and CO from V₉₈ and including the most important quantum corrections. A comparison with experimental data indicates that the V₉₈ PES does not yield complete agreement for the virial coefficient; the van der Waals well of the surface is too deep by 4%-9%, though it represents an improvement over earlier surfaces. The V₉₈ surface has also been used in full coupled-channel cross section and rate coefficient calculations for rotationally inelastic scattering of CO by ground state para- and ortho-H₂ [35]. Mengel *et al.* [32] also reported quantum-scattering calculations to determine inelastic rate coefficients in H₂-CO collisions. However, because the attractive well of V₉₈ is too deep, Mengel *et al.* modified the PES by multiplying the interaction energies by a constant factor of 0.93 which was subsequently used in their scattering calculations.

Recently Jankowski and Szalewicz [26] reported a new H₂-CO PES, referred to as V₀₄. To achieve high accuracy, they used the coupled-cluster method with single, double, and noniterative triple excitations [CCSD(T)] and the supermolecular approach. The V₀₄ surface was calculated on a five-dimensional grid including the dependence on the H-H separation, and the CO molecule was regarded as rigid with the C-O separation set to the value of the C-O distance averaged over the CO ground state vibrational wave function. The PES was then obtained by averaging over the intramolecular vibration of H₂ to obtain a four-dimensional rigid-rotor potential. The correlation part of the interaction energy was obtained from extrapolations based on calculations employing a series of basis sets. An analytical fit of the *ab initio* PES has a global minimum of 93.049 cm⁻¹ at the intermolecular separation

of $7.92 a_0$ for the linear geometry with the C atom pointing toward H_2 . The potential was used to calculate the rovibrational energy levels of the para- and ortho- H_2 -CO complex. The results agree very well with those observed by McKellar [16].

II. RESULTS AND DISCUSSION

The theory for scattering of two linear rigid rotors can be found elsewhere [37, 38]. The calculations presented in this paper were performed by applying both close-coupling (CC) [37] and coupled states (CS) approximations [38]. All the CC and CS calculations reported here were performed using the nonreactive scattering code MOLSCAT [39]. In the present study, we adopted the four-dimensional PESs for the H_2 -CO complex, V_{98} and V_{04} , of Jankowski and Szalewicz [25, 26]. Both potentials have exactly the same long-range relations and coefficients. However, the significant difference between V_{04} and V_{98} is that the new potential has the global well depth of -93.049 cm^{-1} while the old one has a global minima of -109.272 cm^{-1} for the same geometry but at a slightly larger intermolecular distance of $7.76 a_0$. The differences between V_{04} and V_{98} originates from improvements in the *ab initio* calculations for $R < 10 a_0$ as described in [26].

In the quantum scattering calculations, the coupled-channel equations were integrated using the modified log-derivative Airy propagator of Alexander and Manolopoulos [40] with a variable step size. The highest Legendre terms in the potential expansion for H_2 and CO are, respectively, 8 and 10. The numbers of Gauss integration points used in projecting angular components of the potential are 10, 11, 12 for integration in θ_1 , θ_2 , and ϕ , respectively. The propagation was carried out to a maximum intermolecular separation of $R = 60 \text{ \AA}$. Calculations were performed for collision energies between 10^{-6} cm^{-1} and 15000 cm^{-1} in order to evaluate state-to-state rate constants from 10^{-5} to 3000 K. For collision energies larger than 2000 cm^{-1} , the CS method was applied, while the CC approach was used for all other energies. At each energy, a sufficient number of total angular momentum partial waves was included to ensure convergence of the cross sections. The maximum value of the total angular momentum quantum number J employed in the calculations was 300. The rotational basis sets consisted of levels of CO $j_2 \leq 50$ for the cases of scattering with both para- H_2 ($j_1=0, 2$) and ortho- H_2 ($j_1=1, 3$). The rotational constants of H_2 and CO adopted here are 60.853 cm^{-1} and 1.9225 cm^{-1} , respectively. Hereafter, j_1 denotes the rotational

quantum number of H₂, and j_2 for CO.

A. State-to-state cross sections

Antonova *et al.* [17] measured the relative state-to-state rotationally inelastic cross sections for excitation of CO by H₂ in a crossed molecular beam experiment at collision energies of 795, 860, and 991 cm⁻¹. They determined the initial state distribution of CO to have the fractional populations of 0.75 in $j_2=0$ and of 0.25 in $j_2=1$ with a variation of ± 0.05 . There was no direct determination of the initial H₂ rotational distribution. Using CC calculations, we obtained cross sections from initial CO rotational levels in $j_2 = 0$ and $j_2 = 1$ at the same collision energies and calculated the effective cross section using the same fractional populations of CO. The comparison between our calculations and the measurements are shown in Fig. 1. Our CC results for the final CO j'_2 distributions are seen to be in good agreement with experiment, validating the accuracy of V_{04} as well as the present scattering calculations. However, we note that the measured distributions were relative and were normalized to CS calculations using V_{98} [17]. The differences between cross sections obtained with V_{98} and V_{04} are small at these collision energies as will be shown below.

We have performed calculations of the collision energy dependence of state-to-state quenching cross sections for initial rotational states of CO, $j_2=1, 2,$ and 3 , by collisions with both para- and ortho-H₂. Flower [35] employed the MOLCOL quantum scattering code [41] to perform full coupled-channel calculations for H₂-CO on V_{98} . He noticed a series of resonances in the cross sections for rotational quenching $j_2 = 1 \rightarrow j'_2 = 0$ induced by para-H₂ ($j_1=0$). We repeated Flower's calculation, but using the CC method with MOLSCAT. A comparison depicted in Fig. 2 demonstrates that results from the two scattering codes give very good agreement, both revealing similar resonance structure. For collision energies less than ~ 10 cm⁻¹, there is a slight shift to smaller energies for the MOLSCAT results. We note that this shift is very similar to that shown in Fig. 3b of Ref. [42], where MOLSCAT and MOLCOL results are compared for vibrational quenching in H₂-H₂ scattering. The good agreement between the MOLSCAT and MOLCOL results also confirms the accuracy of the current MOLSCAT calculations.

In Fig. 3, we compare the quenching cross sections of CO from $j_2 = 1 \rightarrow j'_2 = 0$ at low collision energies on both V_{98} and V_{04} PESs due to collisions with para-H₂. The cross

sections on both potentials exhibit the threshold behavior predicted by Wigner’s Law [43] at ultra-low collision energies, where only s -wave scattering contributes and the cross sections vary inversely with the relative velocity. In the intermediate energy region, between 10^{-1} and 100 cm^{-1} , the cross sections from both potentials display scattering resonances because of the influence of the attractive region of the interaction potential, but they reveal very different structures. For $\text{H}_2\text{-CO}$, the van der Waals well is deeper than many other collision complexes (e.g., He-H_2 , He-CO) and leads to a more rich resonance structure extending to higher collision energies. As discussed by Reid *et al.* [44], the low collision energy regime fosters the formation of quasi-bound levels or van der Waals complexes. These long-lived complexes allow multiple collisions to occur thereby strongly enhancing the vibrational and rotational relaxation process and also give rise to open-channel (shape) [45] and closed-channel (Feshbach) [46] resonances. Interestingly, the quenching cross section computed on the V_{98} potential in the ultralow energy limit is about a factor of five larger than that obtained using V_{04} . The enhancement of the quenching cross section for the V_{98} potential in the Wigner threshold regime is attributed to the presence of a zero-energy resonance. The existence of the zero-energy resonance in V_{98} is further verified by calculating elastic cross sections for $\text{H}_2(j_1=0)+\text{CO}(j_2=1)$ collisions which are displayed in Fig. 4. Typically, the presence of a zero-energy resonance leads to large values for the limiting elastic cross section. As expected, the results on the V_{98} potential show a steep rise as the energy is decreased from 0.1 to 10^{-3} cm^{-1} . No such feature is seen in the cross sections computed using the V_{04} potential. The limiting value of the elastic cross section on the V_{98} potential is about a factor of five larger than that obtained using the V_{04} potential and the inset reveals that the V_{98} elastic cross section is dominated by s -wave scattering for collision energies less than $\sim 0.02 \text{ cm}^{-1}$. The complex scattering length for $\text{H}_2(j_1=0)+\text{CO}(j_2=1)$ collisions on the V_{98} potential is calculated to be $a_{01} = \alpha_{01} - i\beta_{01} = -23.17 - i(0.357) \text{ \AA}$ where α_{01} and β_{01} are, respectively, the real and imaginary parts of the scattering length. The negative value of the real part of the scattering length implies that the zero-energy resonance is a virtual state. Using the scattering length approximation [47] we estimate the binding energy of the virtual state to be $\sim -0.017 \text{ cm}^{-1}$. However, it must be emphasized that the presence of zero-energy resonances is very sensitive to details of the PESs and it is generally difficult to locate them using traditional bound state calculations. In what follows, we restrict our scattering calculations to the V_{04} PES.

State-to-state cross sections as functions of collision energies for quenching from initial rotational levels of CO, $j_2=1, 2$ and 3 , into the individual final rotational levels ($j'_2=0, 1, 2$) are shown in Fig. 5 and 6 for CO scattering by para- and ortho- H_2 , respectively. Generally, the state-to-state cross sections from different initial j_2 levels have similar structures. Each of the cross sections exhibits the threshold behavior predicted by Wigner's Law at ultra-low energies. In the intermediate energy regime between $\sim 10^{-3}$ – 90 cm^{-1} , the cross sections depict a number of resonances which influence the quenching rate coefficients at low temperatures as shown below. For all quenching cross sections, the resonances occur at about the same collision energy for each initial j_2 level.

In the quenching of $j_2 = 2$, Fig. 5b displays that the Wigner threshold behavior occurs for energies less than 10^{-4} cm^{-1} for $j'_2 = 0$, and for energies less than 10^{-3} cm^{-1} for $j'_2 = 1$. Both cross sections for quenching to $j'_2 = 0$ and 1 have Gaussian-type resonance structures at energies below 0.1 cm^{-1} , but suppressed compared with that for $j_2 = 1 \rightarrow j'_2 = 0$ as shown in Figs. 3 and 5a. The same low-energy resonance feature is seen to decrease further for quenching from $j_2 = 3$ as displayed in Fig. 5c. A similar decrease of shape resonance strength with increasing j was found by Zhu *et al.* [48] for vibrational quenching of $v = 1$ in He-CO collisions and by Yang *et al.* [49] for H-CO scattering. In all cases and over most of the considered energy range, the quenching cross sections are dominated by $\Delta j_2 = -1$ transitions, a trend similar to that noted for the He-CO system [50] where the cross sections increase with decreasing CO rotational energy-gap between initial and final states.

For CO scattering by ortho- H_2 , it can be seen from Fig. 6 that the quenching cross sections are of a similar magnitude as those obtained for para- H_2 . However, the broad Gaussian-type low-energy resonance is significantly suppressed particularly for $j_2 = 1$ and the $j_2 = 3 \rightarrow j'_2 = 1$ transition. The resonances arising from quasibound states of the van der Waals interaction get washed off with increasing initial CO rotation. While this also occurs for para- H_2 collisions, the resonances are not as prominent as those obtained for para- H_2 as shown in Fig. 5. Moreover, unlike para- H_2 results, the magnitudes of cross sections for different Δj_2 transitions do not follow a clear energy-gap law behavior.

B. State-to-state quenching rate coefficients

The state-to-state cross sections of Figs. 5 and 6 were thermally averaged over the kinetic energy distribution to yield state-to-state rate coefficients of CO from specific initial rotational states j_2 as functions of the temperature, T . The quenching rate coefficients at temperatures ranging from 10^{-5} to 3000 K are shown in Fig. 7 and 8 for CO scattering with para- and ortho- H_2 , respectively. Unfortunately, we are unaware of any experimental rate coefficient data for rotational transitions in CO by collisions with H_2 . Therefore, we compare our results with the theoretical results of Flower [35] which were obtained over a limited temperature range of 5 to 400 K with the V_{98} PES. Similar results were obtained earlier by Mengel *et al.* [32].

Considering first quenching rate coefficients for scattering with para- H_2 , it can be seen from Figs. 7a and 7b, that the low-energy Gaussian-type resonance delays the onset of the Wigner threshold regime to temperatures below about 10^{-4} K for $j_2 = 1$ and 2. For $j_2 = 3$, the Wigner regime occurs at higher temperatures due to the suppression of this resonance. Between ~ 1 and 100 K, which is the van der Waals interaction-dominated regime, the rate coefficients exhibit oscillatory temperature dependence due to the presence of resonances. Finally, at temperatures above ~ 500 K the rate coefficients generally increase with increasing temperature. Comparison with Flower's rate coefficients obtained with V_{98} shows that at temperatures higher than ~ 50 K, there is generally good agreement. However, Flower's results are smaller than the present rate coefficients for lower temperatures with the discrepancy increasing with decreasing temperature. Exceptions to this behavior are the transitions $j_2 = 2 \rightarrow j'_2 = 1$ and $j_2 = 3 \rightarrow j'_2 = 0$ which are in good agreement. However, for $j_2 = 3 \rightarrow j'_2 = 1$ and 2 the bump near 20 K in the current rate coefficients are absent from the Flower results likely due to resonances missing from scattering on V_{98} .

For scattering by ortho- H_2 , the trends noted for the cross sections are also evident in the rate coefficients. In particular the suppression of the low-energy Gaussian-type resonance allows for the Wigner regime to set-in at somewhat higher temperatures. However, oscillations due to resonances and a general increase in the rate coefficients above 100 K are similar. Comparisons to the work of Flower are more mixed with the current results being generally smaller than Flower's rate coefficients, contrary to that observed for para- H_2 . There are, however, exceptions such as the quenching transition $j_2 = 3 \rightarrow j'_2 = 2$ where the two sets of

results agree very well over the temperature range where data are available. The differences are likely due to shifts in the energy positions of resonances for scattering on the two PESs. We did not perform ortho-H₂ calculations on V₉₈, nor did Flower present such cross sections.

In general, the comparisons of the current rate coefficients obtained using the V₀₄ potential with Flower’s rate coefficients on the V₉₈ surface show that the agreement is better for CO scattering with para-H₂ than for ortho-H₂ and mostly at higher temperatures. For CO scattering with para-H₂, the discrepancy between the two sets of rate coefficients can be as high as 30%, while for ortho-H₂ the differences reach 60% at some temperatures. We believe that the discrepancies mainly arise from the difference between V₀₄ and V₉₈ potentials and not from the scattering calculations as discussed above.

III. CONCLUSION

Rotational quenching of CO due to para- and ortho-H₂ collisions has been studied using explicit quantum mechanical close-coupling approach and the coupled-states approximation on the potential surfaces, V₉₈ and V₀₄, of Jankowski and Szalewicz. State-to-state quenching cross sections of CO from $j_2=1, 2,$ and 3 show resonance structures at intermediate energies due to the van der Waals well. For CO scattering by para-H₂ the quenching cross sections are dominated by $\Delta j_2 = -1$ transitions. The quenching rate coefficients attain finite values in the limit of zero temperature in accordance with the Wigner threshold law and the resonance structure contributes significantly to the temperature dependence of the rate coefficients. For temperatures less than ~ 50 K, the current state-to-state rotational quenching rate coefficients obtained with V₀₄ are found to depart from the results of Flower, obtained with V₉₈, by as much as 30% and 60% for para- and ortho-H₂ collisions, respectively. The differences are likely related to the reduction in the well-depth of the newer potential which is further illustrated by the shifting of a zero-energy resonance found in V₉₈ to the continuum of the H₂-CO van der Waals complex of V₀₄ which has dramatic effects on the ultra-low energy cross sections.

Acknowledgments

BY and PCS acknowledge support from NASA grant NNG04GM59G. NB acknowledges support from NSF through grant PHY-0245019 and the Research Corporation. RCF acknowledges support from the NSF through grant PHY-0244066 and a grant to ITAMP at Harvard University and Smithsonian Astrophysical Observatory. We thank Dr. Piotr Jankowski for providing his H₂-CO potential subroutine. Some of the calculations were performed on the IBM p655 High Performance Computer of the UGA Research Computing Center. A portion of our implementation of MOLSCAT for H₂-CO was adopted from G. McBane.

-
- [1] A. Schweitzer, P. H. Hauschildt, and E. Baron, *Astrophys. J.* **541**, 1004 (2000).
 - [2] B. T. Draine and F. Bertoldi, *Astrophys. J.* **468**, 269 (1996)
 - [3] G. Shaw, G. J. Ferland, N. P. Abel, P. C. Stancil, and P. A. M. van Hoof, *Astrophys. J.* **624**, 794 (2005).
 - [4] A. Kudian, H. L. Welsh, and A. Watanabe, *J. Chem. Phys.* **47**, 1553 (1967).
 - [5] H. P. Butz, R. Feltgen, H. Pauly, and H. Vehmeyer, *Z. Phys.* **247**, 70 (1971).
 - [6] A. Kuppermann, R. J. Gordon, and M. J. Coggiola, *Faraday Discuss. Chem. Soc.* **55**, 145 (1973).
 - [7] J. P. Bouanich and C. Brodbeck, *J. Quant. Spectrosc. Radiat. Trans.* **13**, 1 (1973).
 - [8] R. B. Nerf, Jr. and M. A. Sonnenberg, *J. Mol. Spectrosc.* **58**, 474 (1975).
 - [9] P. Brechignac, A. Picard-Bersellini, R. Charneau, and J. M. Launay, *Chem. Phys.* **53**, 165 (1980).
 - [10] P. Andresen, H. Joswig, H. Pauly, and R. Schinke, *J. Chem. Phys.* **77**, 2204 (1982).
 - [11] A. Picard-Bersellini, R. Charneau, and P. Brechignac, *J. Chem. Phys.* **78**, 5900 (1983).
 - [12] B. Schramm, E. Elias, L. Kern, G. Natour, A. Schmitt, and C. Weber, *Ber. Bunsenges. Phys. Chem.* **95**, 615 (1991).
 - [13] T. Drascher, T. F. Giesen, T. Y. Yang, N. Schmucker, R. Schieder, G. Winnewisser, P. Joubert, and J. Bonamy, *J. Mol. Spectrosc.* **192**, 268 (1998).
 - [14] A. R. W. McKellar, *J. Chem. Phys.* **93**, 18 (1990).

- [15] A. R. W. McKellar, Chem. Phys. Lett. **186**, 58 (1991).
- [16] A. R. W. McKellar, J. Chem. Phys. **108**, 1811 (1998).
- [17] S. Antonova, A. P. Tsakotellis, A. Lin, and G. C. McBane, J. Chem. Phys. **112**, 554 (2000).
- [18] S. Green and P. Thaddeus, Astrophys. J. **205**, 766 (1976).
- [19] J. Prisetto, E. Kochanski, and D. R. Flower, Chem. Phys. **27**, 373 (1978).
- [20] D. R. Flower, J. M. Launay, E. Kochanski, and J. Prisetto, Chem. Phys. **37**, 355 (1979).
- [21] L. L. Poulsen, Chem. Phys. **68**, 29 (1982).
- [22] R. Schinke, H. Meyer, U. Buck, and G. H. F. Dierksen, J. Chem. Phys. **80**, 5518 (1984).
- [23] Z. Bacić, R. Schinke, and G. H. F. Dierksen, J. Chem. Phys. **82**, 236 (1985).
- [24] Z. Bacic, R. Schinke, and G. H. F. Dierksen, J. Chem. Phys. **82**, 245 (1985).
- [25] P. Jankowski and K. Szalewicz, J. Chem. Phys. **108**, 3554 (1998).
- [26] P. Jankowski and K. Szalewicz, J. Chem. Phys. **123**, 104301 (2005).
- [27] M. C. van Hemert, J. Chem. Phys. **78**, 2345 (1983).
- [28] C. A. Parish, J. D. Augspurger, and C. E. Dykstra, J. Phys. Chem. **96**, 2069 (1992).
- [29] G. Danby, J. Furlong, D. Lodge, S. Miller, and A. Patel, J. Phys. B **26**, 4127 (1993).
- [30] M. C. Salazar, A. de Castro, J. L. Paz, G. H. F. Dierksen, and A. J. Hernandez, Int. J. Quantum Chem. **55**, 251 (1995).
- [31] J. P. Reid, C. J. S. M. Simpson, and H. M. Quiney, J. Chem. Phys. **106**, 4931 (1997).
- [32] M. Mengel, F. C. DeLucia, and E. Herbst, Can. J. Phys. **79**, 589 (2001).
- [33] D. J. Baker and D. R. Flower, J. Phys. B **17**, 119 (1984).
- [34] D. R. Flower and J. M. Launay, Mon. Not. R. astr. Soc **214**, 271 (1985).
- [35] D. R. Flower, J. Phys. B **34**, 2731 (2001).
- [36] J. Gottfried and G. C. McBane, J. Chem. Phys. **112**, 4417 (2000).
- [37] S. Green, J. Chem. Phys. **62**, 2271 (1975).
- [38] T. G. Heil, S. Green, and D. J. Kouri, J. Chem. Phys. **68**, 2562 (1978).
- [39] J. M. Hutson and S. Green, MOLSCAT computer code, version 14, Collaborative Computational Project No. 6 of the Engineering and Physical Sciences Research Council (UK), 1994.
- [40] M. H. Alexander and D. E. Manolopoulos, J. Chem. Phys. **86**, 2044 (1987).
- [41] D. R. Flower, G. Bourhis, and J-M. Launay, Comput. Phys. Commun. **131**, 187 (2000).
- [42] D. R. Flower and E. Roueff, J. Phys. B **23**, 3399 (1999).
- [43] E. P. Wigner, Phys. Rev. **73**, 1002 (1948).

- [44] J. P. Reid, C. J. S. M. Simpson, and H. M. Quiney, *J. Chem. Phys.* **107**, 9929 (1997).
- [45] J. P. Toennies, W. Welz, and G. Wolf, *J. Chem. Phys.* **71**, 614 (1979).
- [46] D. A. Micha, *Phys. Rev.* **162**, 88 (1967).
- [47] N. Balakrishnan, V. Kharchenko, R. C. Forrey, and A. Dalgarno, *Chem. Phys. Lett.* **280**, 5 (1997).
- [48] C. Zhu, N. Balakrishnan, and A. Dalgarno, *J. Chem. Phys.* **115**, 1335 (2001).
- [49] B. Yang, P. C. Stancil, and N. Balakrishnan, *J. Chem. Phys.* **123**, 094308 (2005).
- [50] E. Bodo, F. A. Gianturco, and A. Dalgarno, *Chem. Phys. Lett.* **353**, 127 (2002).

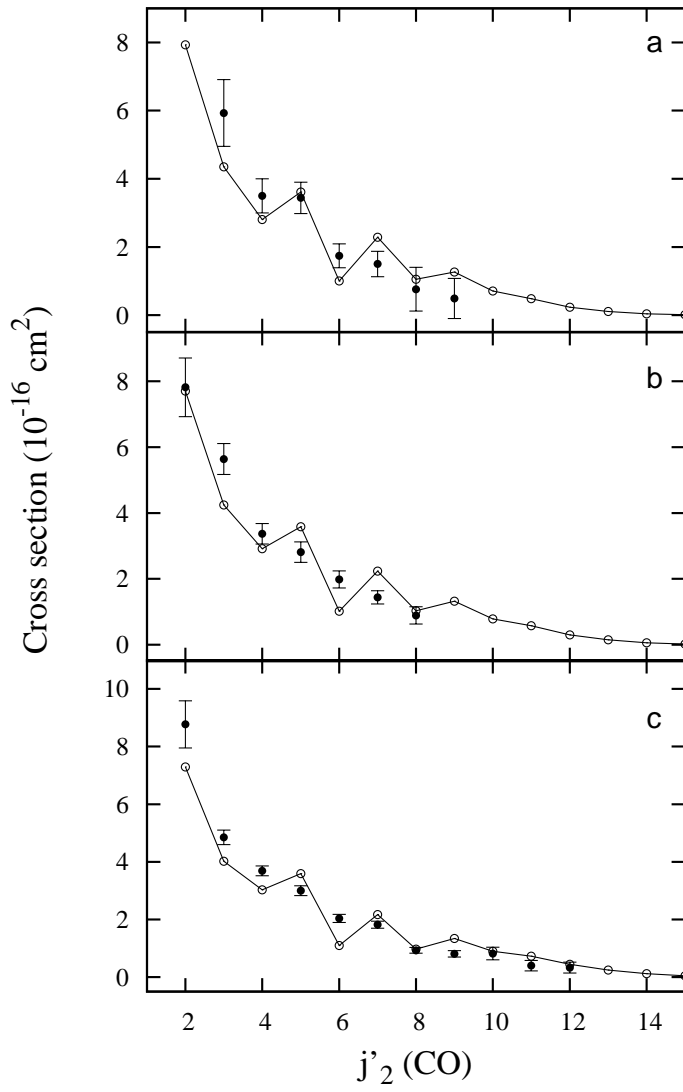


FIG. 1: State-to-state cross sections for rotational excitation of CO by collisions with H₂, compared with experimental results for collision energies: (a) 795 cm⁻¹, (b) 860 cm⁻¹, (c) 991 cm⁻¹. Line with open circles: current CC calculations; solid circles with error bars: measurements [17].

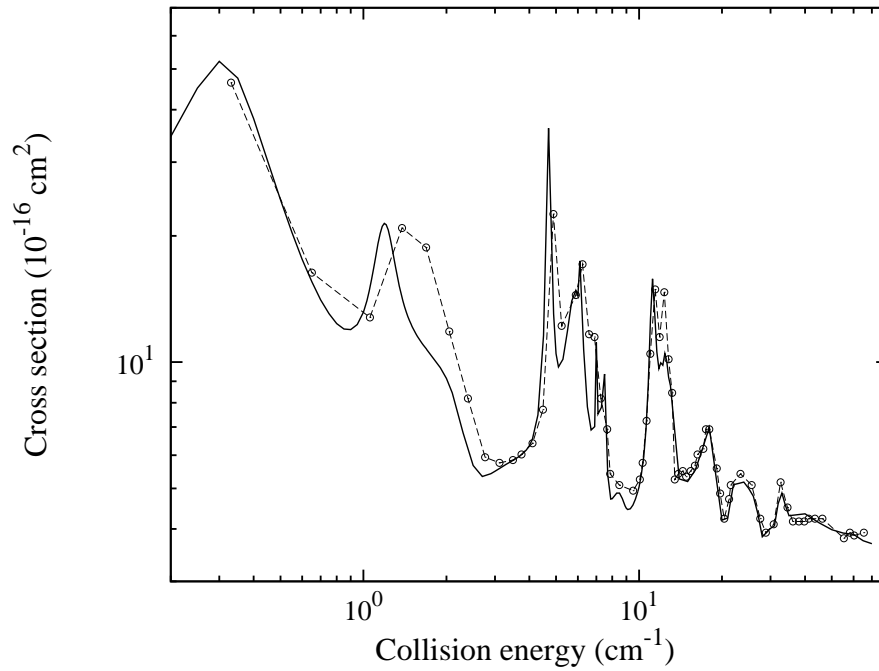


FIG. 2: Quenching cross sections of $\text{CO}(j_2 = 1)$ by collisions with para- H_2 ($j_1 = 0$) as functions of collision energy obtained using the V_{98} PES. Solid line: current CC calculations; dashed line with open circles: Flower [35].

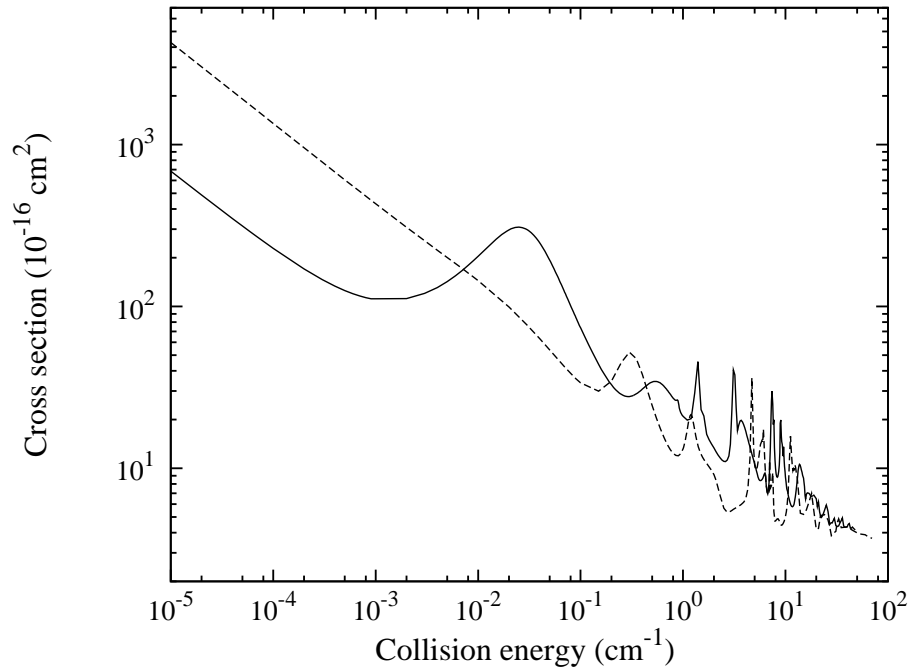


FIG. 3: Cross sections for the quenching of $\text{CO}(j_2 = 1)$ by collisions with para- H_2 ($j_1 = 0$) as functions of collision energy evaluated using the V_{98} and V_{04} PESs. Solid line: CC calculations on V_{04} ; dashed line: CC calculations on V_{98} .

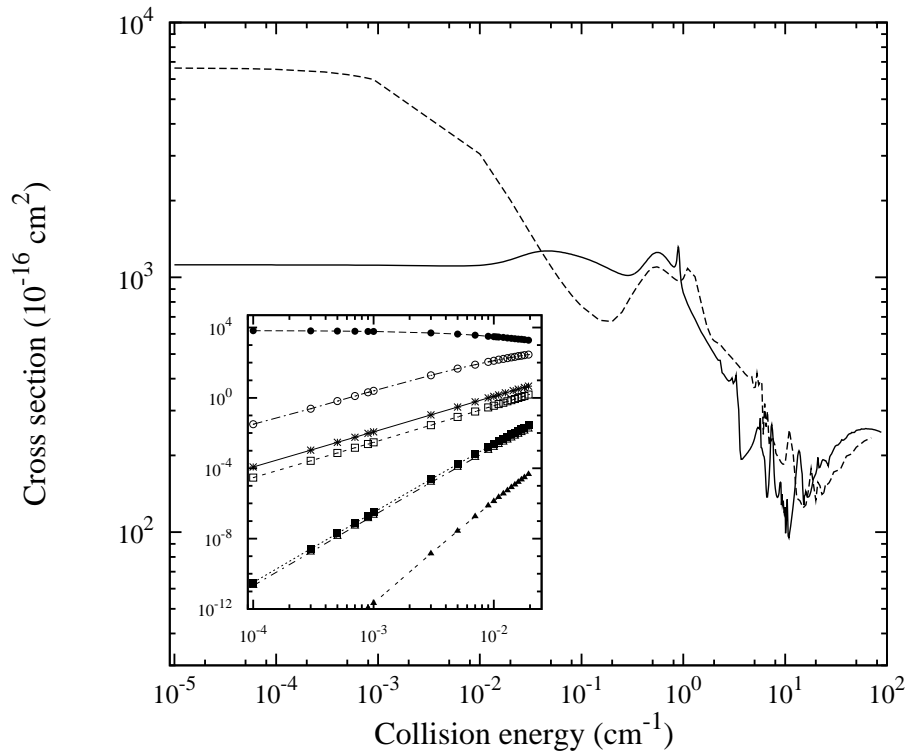


FIG. 4: Elastic scattering cross sections of CO ($j_2=1$) in collisions with para- H_2 ($j_1=0$) as functions of collision energy. Solid line: CC calculations on V_{04} ; dashed line: CC calculations on V_{98} . Inset: J, l-resolved partial elastic cross sections for V_{98} , line with stars: $J=0, l=1$; line with solid circles: $J=1, l=0$; line with open squares: $J=1, l=1$; line with solid squares: $J=1, l=2$; line with open circles: $J=2, l=1$; line with open triangles: $J=2, l=2$; line with solid triangles: $J=2, l=3$.

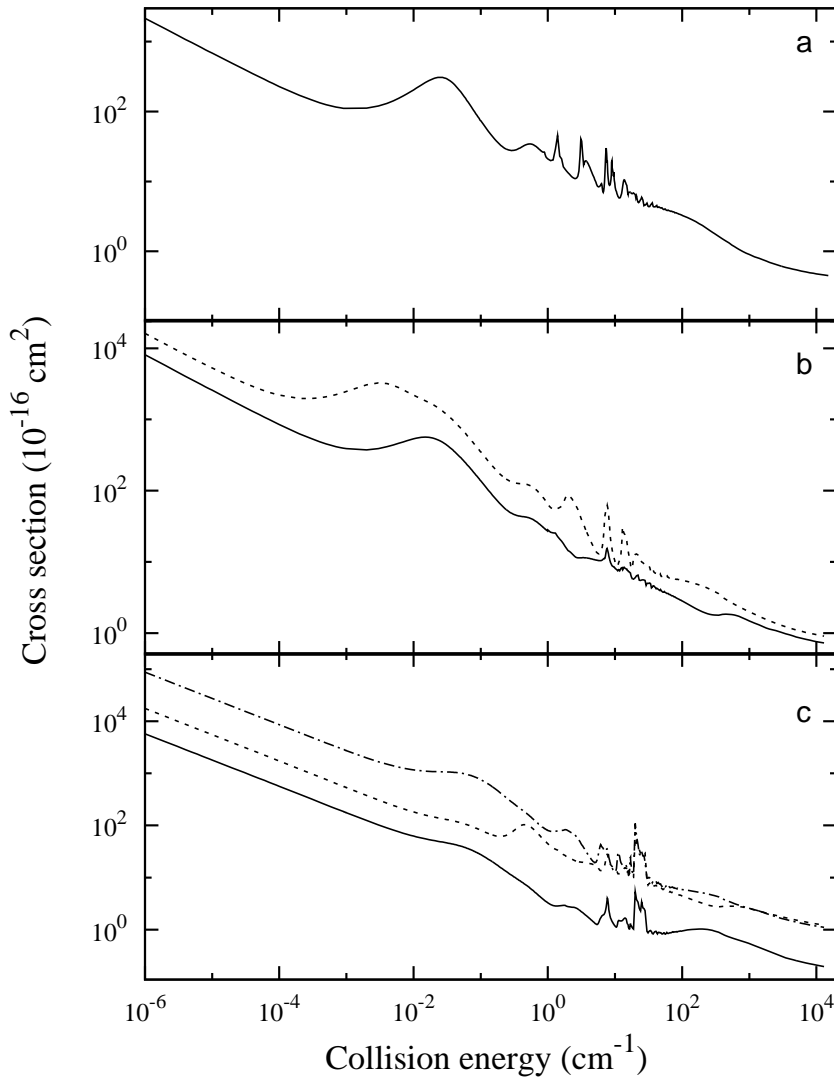


FIG. 5: Cross sections for the quenching of $\text{CO}(j_2)$ by collisions with para- H_2 ($j_1 = 0$) as functions of collision energy evaluated using the V_{04} PES: (a) $j_2 = 1 \rightarrow j'_2 = 0$; (b) solid line: $j_2 = 2 \rightarrow j'_2 = 0$, dashed line: $j_2 = 2 \rightarrow j'_2 = 1$; (c) solid line: $j_2 = 3 \rightarrow j'_2 = 0$, dashed line: $j_2 = 3 \rightarrow j'_2 = 1$, dash dotted line: $j_2 = 3 \rightarrow j'_2 = 2$.

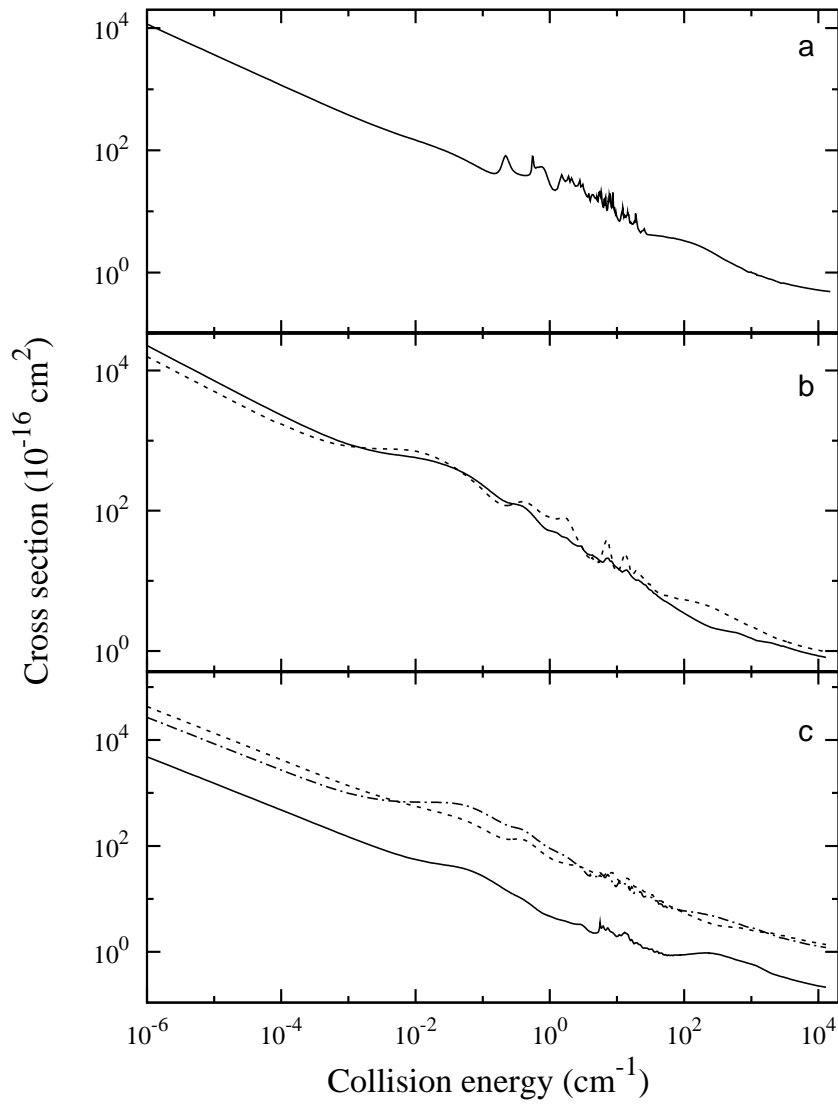


FIG. 6: Same as Fig. 5, except for CO scattering with ortho-H₂($j_1 = 1$).

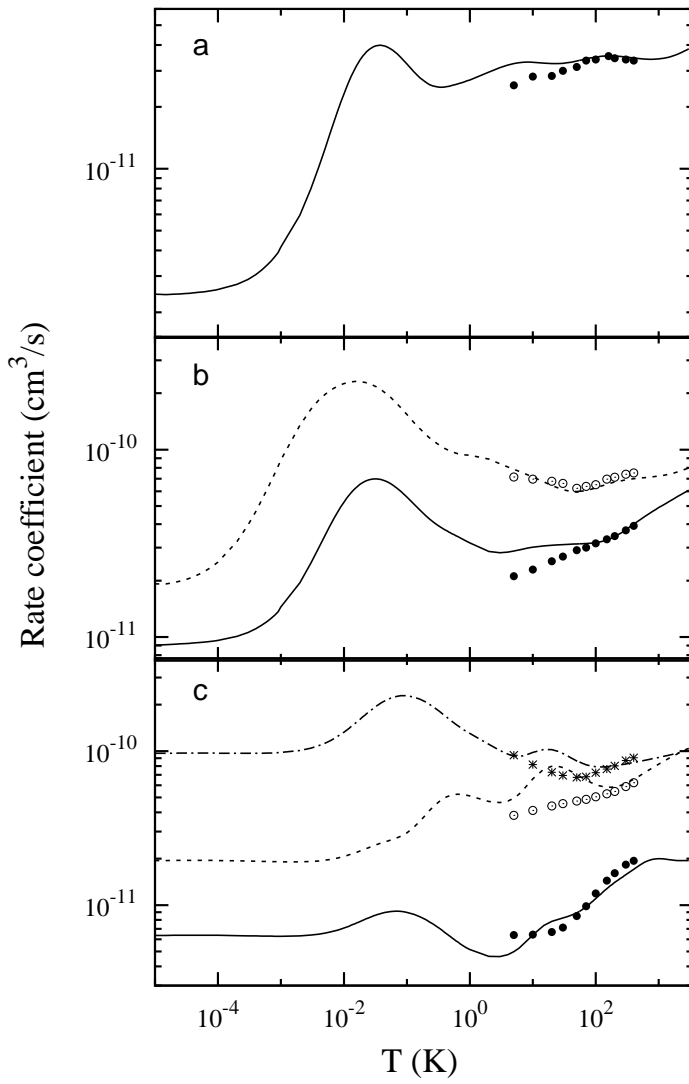


FIG. 7: Rate coefficients for the quenching of $\text{CO}(j_2)$ by collisions with para- $\text{H}_2(j_1 = 0)$ as functions of the temperature. Lines indicate current calculations on potential V_{04} , symbols denote Flower's results [35] on potential V_{98} : (a) $j_2 = 1 \rightarrow j'_2 = 0$. (b) solid line: $j_2 = 2 \rightarrow j'_2 = 0$, dashed line: $j_2 = 2 \rightarrow j'_2 = 1$, solid circles: $j_2 = 2 \rightarrow j'_2 = 0$, open circles: $j_2 = 2 \rightarrow j'_2 = 1$; (c) solid line: $j_2 = 3 \rightarrow j'_2 = 0$, dashed line: $j_2 = 3 \rightarrow j'_2 = 1$, dash dotted line: $j_2 = 3 \rightarrow j'_2 = 2$, solid circles: $j_2 = 3 \rightarrow j'_2 = 0$, open circles: $j_2 = 3 \rightarrow j'_2 = 1$, stars: $j_2 = 3 \rightarrow j'_2 = 2$.

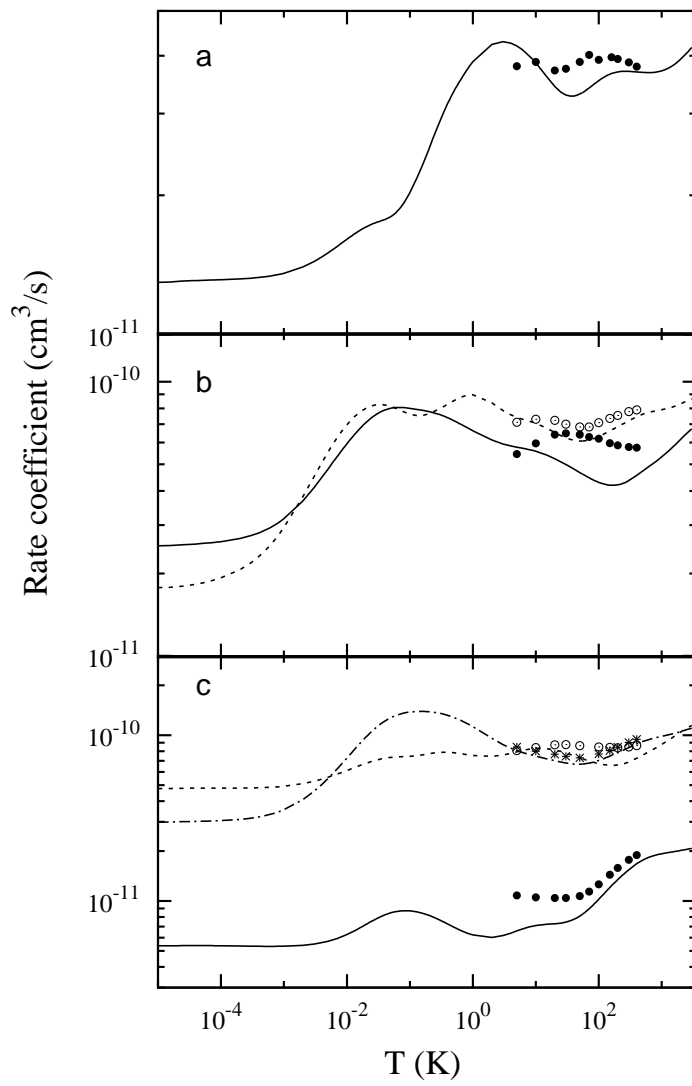


FIG. 8: Same as Fig. 7, except for CO collisions with ortho- $\text{H}_2(j_1 = 1)$.